INFLUENZA IMMUNOLOGY

Antibody landscapes after influenza virus infection or vaccination

J. M. Fonville,[1,2,3]* S. H. Wilks,[1,2]* S. L. James,[1,2] A. Fox,[4] M. Ventresca,[1]† M. Aban,[5] L. Xue,[5] T. C. Jones,[1,2] Le N. M. H.,[4] Pham Q. T.,[6] Tran N. D.,[6] Y. Wong,[7] A. Mosterin,[1,2] L. C. Katzelnick,[1,2] D. Labonte,[8] Le T. T.,[6] G. van der Net,[3] E. Skepner,[1,2] C. A. Russell,[2,9] T. D. Kaplan,[10] G. F. Rimmelzwaan,[3] N. Masurel,[3]‡ J. C. de Jong,[3] A. Palache,[11] W. E. P. Beyer,[3] Le Q. M.,[6] Nguyen T. H.,[6] H. F. L. Wertheim,[4,12] A. C. Hurt,[5,13] A. D. M. E. Osterhaus,[3] I. G. Barr,[5] R. A. M. Fouchier,[3] P. W. Horby,[4,12] D. J. Smith[1,2,3]§

We introduce the antibody landscape, a method for the quantitative analysis of antibody-mediated immunity to antigenically variable pathogens, achieved by accounting for antigenic variation among pathogen strains. We generated antibody landscapes to study immune profiles covering 43 years of influenza A/H3N2 virus evolution for 69 individuals monitored for infection over 6 years and for 225 individuals pre- and postvaccination. Upon infection and vaccination, titers increased broadly, including previously encountered viruses far beyond the extent of cross-reactivity observed after a primary infection. We explored implications for vaccination and found that the use of an antigenically advanced virus had the dual benefit of inducing antibodies against both advanced and previous antigenic clusters. These results indicate that preemptive vaccine updates may improve influenza vaccine efficacy in previously exposed individuals.

Much of the global burden of infectious disease today is caused by antigenically variable pathogens, which escape immunity induced by prior infection or vaccination by changing the molecular structure recognized by antibodies. Human influenza viruses are notorious for their capacity to evolve and evade the adaptive immune response. This evolution has been progressive and stepwise (*1*), with antigenically similar viruses circulating for a few years before strains with related but novel antigenic characteristics replace them (*2*) (figs. S1 and S2). As a result, vaccine strain updates, based on analyses of circulating viruses, are necessary to maintain vaccine effectiveness.

[1]Center for Pathogen Evolution, Department of Zoology, University of Cambridge, Cambridge CB2 3EJ, UK. [2]World Health Organization (WHO) Collaborating Center for Modeling, Evolution, and Control of Emerging Infectious Diseases, Cambridge CB2 3EJ, UK. [3]Department of Viroscience, Erasmus Medical Center, Rotterdam 3015 CE, Netherlands. [4]Oxford University Clinical Research Unit and Wellcome Trust Major Overseas Programme, Hanoi, Vietnam. [5]WHO Collaborating Centre for Reference and Research on Influenza, Victorian Infectious Diseases Reference Laboratory at the Peter Doherty Institute for Infection and Immunity, Melbourne VIC 3000, Australia. [6]National Institute of Hygiene and Epidemiology, Hanoi, Vietnam. [7]Oxford University Museum of Natural History, Oxford OX1 3PW, UK. [8]Insect Biomechanics Group, Department of Zoology, University of Cambridge, Cambridge CB2 3EJ, UK. [9]Department of Veterinary Medicine, University of Cambridge, Cambridge CB3 0ES, UK. [10]bobblewire.com, Saint Louis, MO 63112, USA. [11]Abbott Laboratories, Weesp 1380 DA, Netherlands. [12]Nuffield Department of Clinical Medicine, Centre for Tropical Medicine, University of Oxford, Oxford OX3 7BN, UK. [13]Melbourne School of Population and Global Health, University of Melbourne, Parkville VIC 3010, Australia. *These authors contributed equally to this work. †Present address: School of Industrial Engineering, Purdue University, West Lafayette, IN 47907 USA. ‡Deceased. §Corresponding author. E-mail: dsmith@zoo.cam.ac.uk

The current strategy for vaccine strain selection is to choose a virus that is antigenically representative of circulating viruses, mostly determined by using the hemagglutination inhibition (HI) assay to test a global selection of virus isolates against a panel of ferret antisera (*3*). The ferrets used in such studies are naïve to influenza before inoculation, and each antiserum has been raised by infection with only a single virus. Such postinoculation ferret antisera provide well-understood data for the characterization of antigenic differences between influenza viruses (*2*, *4*). However, this strategy does not account for the influence of prior immunity on the response induced by the vaccine when administered to humans.

The direct analysis of human serological data presents an opportunity to assess and understand immune responses in the context of differing background immunity and to use this information as the basis for improved vaccine strain selection and evaluation. Indeed, such data are already used to some extent in the vaccine strain selection process. Unfortunately, immunological patterns in human serological data are difficult to interpret because of complex, and usually unknown, exposure histories and the confounding factor of cross-reactivity due to antigenic relationships among strains. As a result, in-depth analyses of serological data have been difficult, and despite excellent cross-sectional seroepidemiology (*5*), our understanding of the typical characteristics of the human serological response to infection and vaccination has remained limited.

Results from the original (and seminal) studies on the antibody-mediated immune response to influenza virus infection and vaccination in humans (*6*–*9*) have often been interpreted as "original antigenic sin"—a hypothesis that proposes an anamnestic reinforcement of the level of antibody to the strain that first infected the individual that dampens the serologic response to the current virus (*9*–*11*). However, this definition is far from concrete, and the historical literature on the effect of immune memory on the generation of responses to variant antigens has been particularly equivocal.

To increase our ability to quantitatively study human serological data of antigenically variable pathogens, we present a methodology that enables detailed analyses and visualization of complex serological data by plotting antibody-mediated immunity as a function of the antigenic relationships among viruses. To achieve this, we first used antigenic cartography (*2*) to determine the antigenic relationships among a selection of 81 viruses spanning 43 years of influenza A/H3N2 evolution, using HI titrations of first-infection ferret sera (Fig. 1A, fig. S2, and tables S1 and S9). Human serum samples were then titrated against the same viruses and their HI titers plotted in an extra dimension added to the antigenic map (Fig. 1B).

We found that HI titers of a given serum are related for antigenically similar viruses (fig. S3), and thus a representative smooth surface could be fitted through these HI titers. The resulting antibody landscape represents an immune profile for each serum with elevations corresponding to regions in the antigenic map with higher antibody levels (figs. S4 and S5). Because the landscape at any given point is a function of surrounding data points, antibody levels can be inferred for viruses not included in the titration set. For antibody landscapes of influenza A/H3N2 based on the HI assay, we found that the landscape predicted omitted HI titers with a root mean square error of 1.3 $\log_2$ units, compared with an estimated error arising from HI assay repeatability alone of 0.9 (table S11 and figs. S6 to S11, S13, and S14).

To aid the visual comparison of multiple landscapes, we used a path on the antigenic map that passes through each antigenic cluster in chronological order (Fig. 1C). The corresponding values of the landscape along this summary path were used to represent the three-dimensional landscape in two dimensions (Fig. 1D and fig. S12).

We used this methodology to study serological data we generated from samples taken annually between 2007 and 2012 from unvaccinated individuals in the Ha Nam household cohort study in Vietnam (*12*). More than 10,000 HI titrations were performed to construct a total of 324 landscapes for 69 individuals born between 1917 and 2005, allowing us to assess the serological changes over time (Fig. 2, tables S3 and S4, and fig. S15). Titers were highest for influenza viruses that circulated when an individual was ~6 years old (figs. S42 and S43), corresponding with the time frame of first infection (*13*). Antibody levels against newly circulating viruses tended to be lower than those against strains circulating earlier in an individual's lifetime, as reported previously (*5*, *7*–*9*, *11*). In addition, previous results reported some cross-reactivity to

Downloaded from www.sciencemag.org on March 20, 2015

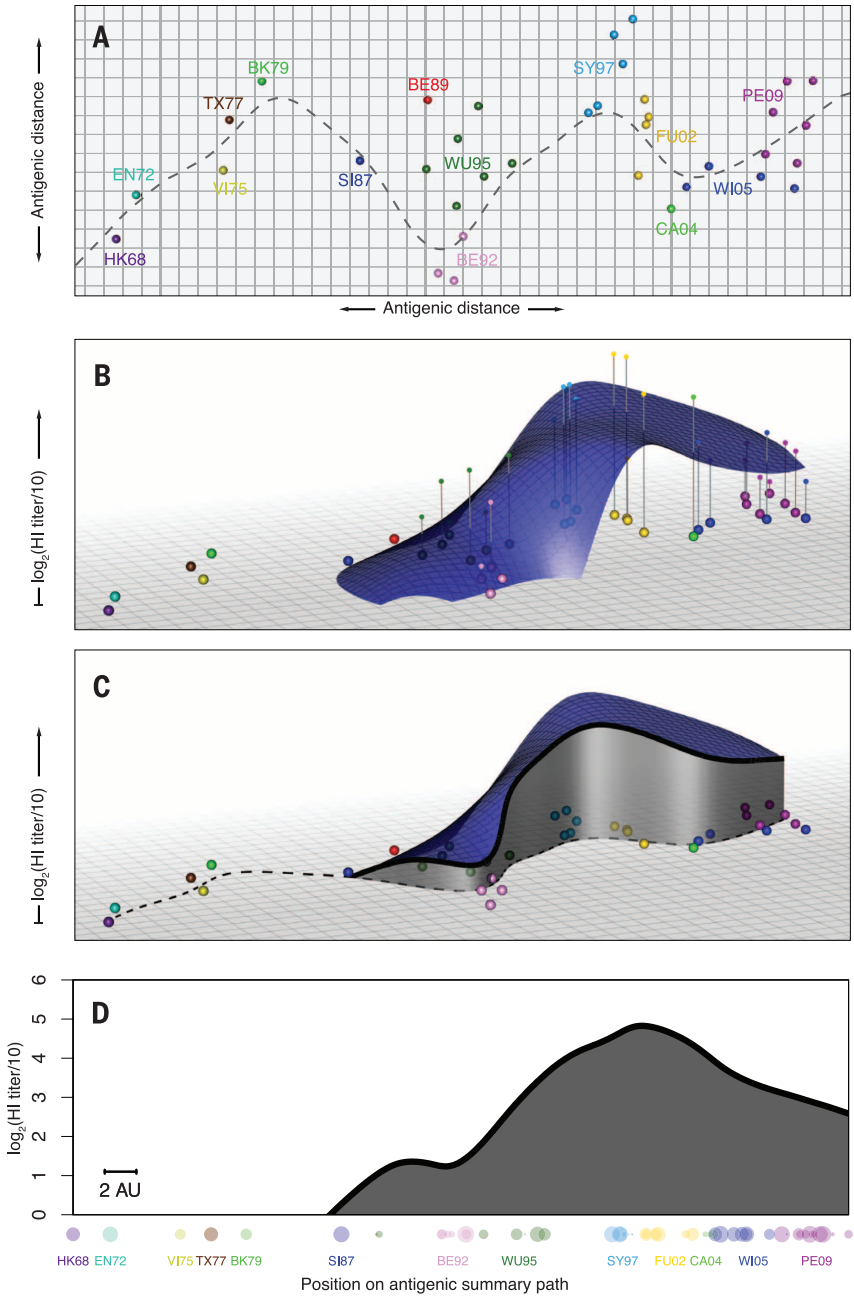

Fig. 1. Creating an antibody landscape. (**A**) Antigenic map of A/H3N2 showing virus strains color-coded by antigenic cluster. Both axes represent antigenic distance, and the spacing between grid lines is 1 antigenic unit, corresponding to a twofold dilution of antiserum in the HI assay. Two units correspond to fourfold dilution, three units to eightfold dilution, and so on (*2*). The gray dashed line shows a path through the antigenic clusters in chronological order calculated by fitting a smoothing spline (*1*). EN72, England 1972; VI75, Victoria 1975; TX77, Texas 1977; BK79, Bangkok 1979; SI87, Sichuan 1987; BE89, Beijing 1989; BE92, Beijing 1992; FU02, Fujian 2002; CA04, California 2004. (**B**) An additional dimension indicates the measured antibody titers as vertical impulses, and a smooth surface is fitted using locally weighted multiple linear regression to create the antibody landscape within the convex hull bounded by the viruses titrated (root mean square error of fit = 1.23 HI $\log_2$ units). (**C**) The height of the landscape along the path in (A) shows a slice through the landscape (*1*). (**D**) The height of the landscape along the antigenic summary path in (C) is plotted to create a rotation-independent two-dimensional summary visualization of the landscape. Titrated virus strains are shown in their corresponding positions along the *x* axis. The symbol radius is inversely proportional to the antigenic distance from the path; symbol color indicates antigenic cluster. The scale bar denotes 2 antigenic units (AU).

strains that circulated before an individual's birth (*5*, *7*–*9*, *14*), and based on the extent of detectable titers to viruses in circulation only before an individual's birth, we quantified this antibody cross-reactivity to be up to two antigenic clusters (table S12). There was substantial heterogeneity among the antibody landscapes of different individuals; however, each individual's landscape shape was typically stable from one year to the next and had distinctive individual features [within-person correlation coefficient r = 0.86 (SD ± 0.22); between-person r = 0.28 ± 0.21 (figs. S16 to S20)].

Infection with A/H3N2 resulted in a notably broad antibody response (Fig. 2 and figs. S21 and S22) that was typically governed by the extent of the preexposure antibody landscape (fig. S45). This antibody response far exceeded the extent of cross-reactivity typically produced in the response after primary exposure with one of the circulating viruses (figs. S44 and S47). For example, an individual born in 1970 and infected in 2009 (Fig. 2, fourth row) had a substantial long-distance response back to the Hong Kong 1968 (HK68) antigenic cluster and all clusters in between, even though these older viruses had not circulated for decades. To illustrate the substantial breadth of this "back-boost," there have been 13 antigenic cluster transitions from HK68 until Perth 2009 (PE09), each ~4.5 antigenic units (corresponding to a 24-fold dilution of antiserum in the HI assay). These antigenic changes have necessitated more than 20 vaccine strain updates and are the result of changes in 69 of the 346 amino acid positions in the HA1 domain of the hemagglutinin gene between HK68 and the PE09 vaccine strain, including substitutions in all of the seven key antigenic positions identified by Koel *et al.* (*15*).

Because of the range of this response and its dependence on the preexposure antibody landscape, we call it a "back-boost." The magnitude of back-boost response declined with antigenic distance from the likely infecting virus (fig. S46). Although the response to older viruses was substantial, titer increases were largest for viruses from the contemporary antigenic cluster, in contrast to a common interpretation of the original antigenic sin hypothesis (fig. S47). Infections with influenza B, A/H1N1, and A/H1N1(pdm09) often caused negligible changes in the A/H3N2 antibody landscape (fig. S23), indicating that the back-boost is specific to virus type and subtype.

Typically, the broad initial response was followed by a period of titer decay during which antibody titers stabilized to form an altered antibody landscape over the course of ~1 year (fig. S24). Comparison of the antibody landscapes of 2007 and 2012 (Fig. 2) shows that the antigenic region for which increased titers were maintained long-term was substantially narrower than that of the initial response to infection. This long-term persistence of increased antibody titers was more specific to the antigenic region of the likely infecting strain but still spanned multiple antigenic clusters (fig. S46).

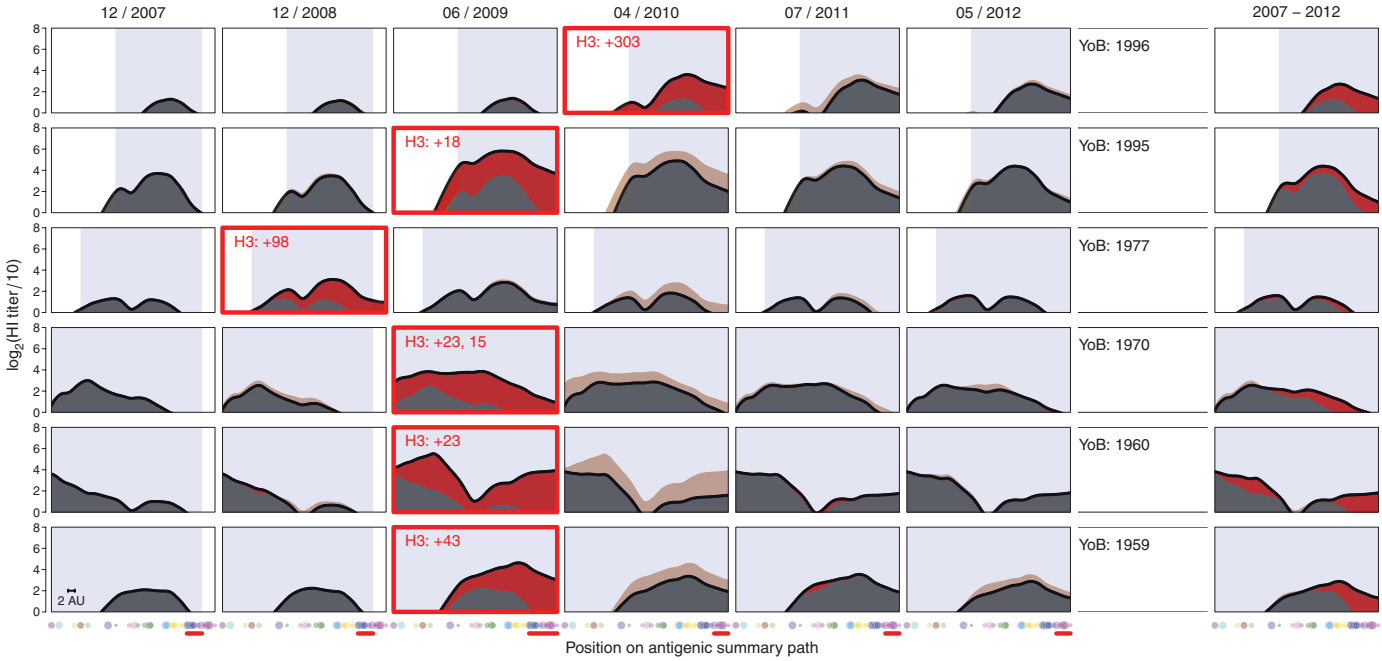

Fig. 2. Antibody landscapes from 2007 to 2012 for six individuals. The black lines represent the landscape height for each position on the antigenic summary path through the antigenic clusters from Fig. 1A. The first sample taken after a confirmed A/H3N2 influenza virus infection is marked with a red box, and the red number gives the days from the date of influenza-like illness–associated swab collection to serum collection. Red shading indicates increases, and beige decreases, compared with the previous year. The blue shaded rectangles indicate antigenic clusters that circulated during an individual's life span until sample collection (table S10). Dots along the *x* axis indicate the subset of 30 viruses used to generate these landscapes; contemporary strains, probably causing the infection, are indicated with red horizontal bars (table S2). The rightmost column shows the difference between the landscape in 2012 compared with 2007. The scale bar indicates 2 antigenic units. YoB, year of birth.

Next we investigated whether the back-boost observed after infection could be used to improve vaccine effectiveness. In the vaccine strain selection process, it is sometimes unclear whether currently circulating strains or antigenically novel strains are most likely to predominate in the next influenza season. The resulting dilemma is whether it is more beneficial to leave the vaccine strain unchanged or to preemptively update the vaccine to match a novel strain, without certainty over which antigenic cluster of viruses will actually circulate.

It would take a large, prospective, multiyear clinical trial comparing the two vaccination approaches to answer these questions definitively. However, we were able to retrospectively test the approach with the sera of 225 human vaccine recipients from two annual influenza vaccine reregistration studies, by identifying an antigenic cluster transition for which there was little circulation of the new cluster before a novel vaccine strain was first tested. Both groups had therefore received antigenically different vaccines, and yet there was no significant difference in the average prevaccination antibody landscapes of the two studies (figs. S30 and S31). Individuals in the first study (n = 102) (table S7), performed in 1997, received the A/Nanchang/933/95 vaccine from the Wuhan 1995 (WU95) antigenic cluster to which there had been some prior exposure, whereas individuals in the 1998 study (n = 123) (table S8) received the A/Sydney/5/97 vaccine from the antigenically advanced Sydney 1997 (SY97) cluster to which there was substantially less prevaccination immunity, thus mimicking a preemptive update.

Individual antibody landscapes were constructed from serum samples taken before vaccination and 4 weeks after vaccination (figs. S25 and S26 and tables S5 and S6) and combined to give overall pre- and postvaccination antibody landscapes (Fig. 3, A and B). As expected after a vaccine update, average vaccination responses were significantly greater against later antigenic clusters after vaccination with the antigenically advanced SY97 strain (figs. S32 to S35). The back-boost after infection was also observed for the vaccination studies, and interestingly, the magnitude and breadth of the response to infection and vaccination were comparable (figs. S27 to S29). The back-boost in the SY97 vaccine study resulted in a slightly larger response to WU95 viruses than the response in the WU95 vaccine study (Fig. 3C). These findings also held when studying only elderly individuals (fig. S36) and individuals with a low prevaccination titer against WU95, typically considered the most susceptible (figs. S37 and S38) (*16*). We further tested a subset of vaccination sera with a neutralization assay, and these data support the results from the HI assay (figs. S40 and S41). Despite differences in prevaccination landscapes, a second study of the Wisconsin 2005 (WI05)–PE09 cluster transition also demonstrated a similar back-boost upon vaccination (fig. S39 and tables S13 and S14).

The mechanism behind the broad back-boost is currently unknown, but we considered several hypotheses (*1*). In summary, rather than a result of the production of novel antibodies with extensive cross-reactivity, the back-boost appears most consistent with memory cell stimulation and antibody recall. This pattern of recall is consistent with raw data from mid–20th century studies on the response to infection or vaccination: Studies on antigenically different A/H1N1 strains also show a broad subtype-specific back-boost (*6*, *8*, *9*). However, this phenomenon was never quantified and put in relation to the antigenic difference among the viruses.

Whether the original antigenic sin hypothesis refers to higher preexposure antibody titers or also to a higher response to the first infecting virus is unclear, and both interpretations have been used over the past 60 years (*17*). We found no evidence for a predisposition in the antibody response toward the likely first infecting strain, and instead we demonstrate that the increase in antibody titers is greatest to the most recently encountered strain. We do, however, corroborate the finding that preexposure antibody reactivity tends to be highest against strains encountered earlier in life (figs. S42 and S43) (*5*, *7*–*9*, *11*). The presence of higher preexposure static titers, but not higher dynamic responses, to the first infecting strain may explain seemingly contradictory reports whereby cross-sectional studies have tended to describe a serological bias supportive of the original antigenic sin dogma (*5*, *11*),

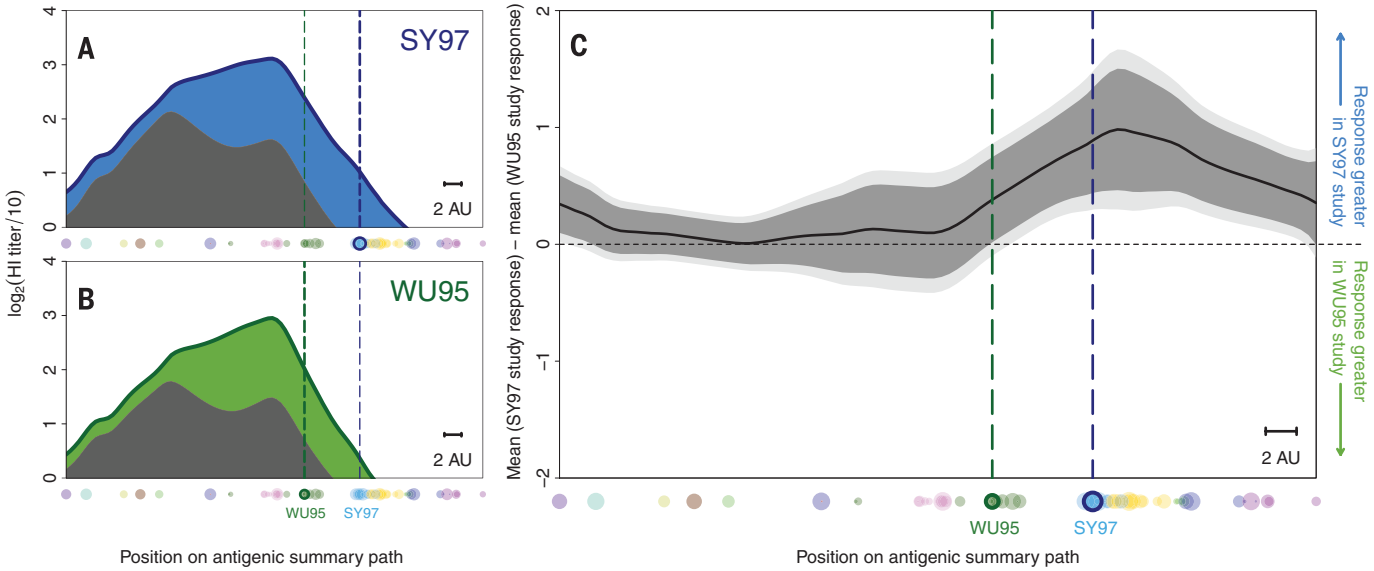

Fig. 3. Comparison of two different vaccines. (**A**) The mean prevaccination landscape (gray) and landscape after vaccination with A/Sydney/5/97 (blue) in the 1998 study (123 individuals) or (**B**) with A/Nanchang/933/95 (green) in the 1997 study (102 individuals) for each position on the antigenic summary path. Dots along the *x* axes indicate the subset of 70 viruses used to generate these landscapes. The vertical dotted lines indicate the position of the SY97 (blue) and WU95 (green) wild-type vaccine viruses. (**C**) Comparison of titer increase after vaccination with A/Nanchang/933/95 or A/Sydney/5/97 for each position along the antigenic summary path. When above the horizontal midpoint, the black line indicates a higher response in the group vaccinated with A/Sydney/5/97; when below the midpoint, it denotes a higher response in the group vaccinated with A/Nanchang/933/95. Data were calculated from the average titer increase between each individual's paired pre- and postvaccination titers, with 95% (dark gray) and 99% (light gray) *t* test–based confidence intervals. Scale bars indicate 2 antigenic units.

whereas investigations into actual responses upon exposure frequently oppose it (*17*, *18*).

These findings also shed light on the growth of the serological immunity over time. Although responses were often present against the oldest strains, these long-distance back-boosts were typically not maintained beyond a year (Fig. 2, rightmost panels, and fig. S24). This is evidence against the hypothesis of long-term and progressive reinforcement of antibody titers against earlier viruses upon exposure to each subsequent antigenic variant over time. Instead, the pattern of higher static titers against antigenic clusters encountered early in life may also be explained if the immune response to primary exposure is larger than the responses to subsequent exposures (fig. S48).

As others have speculated, it is plausible that the decreased antibody responses to subsequent exposures may be a result of "antigen trapping," a hypothesis according to which binding of antigen by preexisting cross-reactive antibodies and memory cells decreases the antigenic load available for priming naïve B cells and leads to a diminished novel response (*5*, *7*, *10*, *19*, *20*). This would also explain why the closest antigenic match between the vaccine strain and the circulating strains does not necessarily generate the best antibody response against the corresponding cluster: The mismatch of an antigenically advanced strain is compensated for by a greater novel response, as a result of reduced antigen trapping (*21*). The extent of interference by antigen trapping on the novel antibody response depends on the degree of antigenic relatedness and prior immunity (*22*). When individuals have no prior immunity to a subtype (such as young children, or in a pandemic), the best vaccine is probably the closest antigenic match, as there will be no prior immunity to avoid and no back-boost to exploit.

These findings highlight potentially important differences between the two types of vaccine mismatch in populations with prior immunity. Following a mismatch due to a delayed vaccine update (in which the vaccine strain, selected 10 to 14 months before the season in which it is used, lags behind influenza virus evolution), neither preexisting nor newly induced antibodies provide immunity against the novel strains. Consequently, such vaccines have poor effectiveness in this mismatch situation (*23*–*26*). However, if there was a vaccine mismatch due to an incorrectly timed, preemptive antigenic update of the vaccine, then the data from our retrospective surrogate study indicate that the extensive back-boost would still induce equivalent titers against previous antigenic strains. Such vaccines would have the dual advantage of being effective against the antigenically novel viruses to which they were targeted while remaining effective, or being even more effective, for contemporary viruses if they continued to circulate.

Our results underscore the importance of accounting for antigenic variation to better understand multiexposure sera; further, we provide a methodology for the direct visualization of otherwise complex serological patterns, allowing basic insights into the breadth of the adaptive humoral immune response to influenza and other antigenically variable pathogens. Antibody landscapes will be useful for the evaluation of evolutionary selection pressures (fig. S49) and the evaluation of different vaccination techniques, including the effect of adjuvants; vaccine composition; dose sparing; and the durability, breadth, and magnitude of responses to universal vaccines. Our results indicate that preemptive vaccine updates may substantially improve influenza vaccine effectiveness in previously exposed individuals. Prospective clinical trials will further test the breadth and longevity of the immunological response and protection provided by antigenically advanced vaccine strains.

REFERENCES AND NOTES

1. Materials and methods are available as supplementary materials on *Science* Online.
2. D. J. Smith *et al.*, *Science* **305**, 371–376 (2004).
3. G. K. Hirst, *J. Exp. Med.* **75**, 49–64 (1942).
4. I. G. Barr *et al.*, *Vaccine* **28**, 1156–1167 (2010).
5. J. Lessler *et al.*, *PLOS Pathog.* **8**, e1002802 (2012).
6. F. L. Horsfall, E. R. Rickard, *J. Exp. Med.* **74**, 433–439 (1941).
7. A. V. Hennessy, F. M. Davenport, T. Francis Jr., *J. Immunol.* **75**, 401–409 (1955).
8. F. M. Davenport, A. V. Hennessy, T. Francis Jr., *J. Exp. Med.* **98**, 641–656 (1953).
9. F. M. Davenport, A. V. Hennessy, *J. Exp. Med.* **104**, 85–97 (1956).
10. S. F. de St. Groth, R. G. Webster, *J. Exp. Med.* **124**, 331–345 (1966).
11. T. Francis Jr., *Proc. Am. Philos. Soc.* **104**, 572–578 (1960).
12. P. Horby *et al.*, *Am. J. Epidemiol.* **175**, 1062–1074 (2012).
13. R. Bodewes *et al.*, *Clin. Vaccine Immunol.* **18**, 469–476 (2011).
14. F. M. Davenport, A. V. Hennessy, C. H. Stuart-Harris, T. Francis Jr., *Lancet* **266**, 469–474 (1955).
15. B. F. Koel *et al.*, *Science* **342**, 976–979 (2013).
16. L. Coudeville *et al.*, *BMC Med. Res. Methodol.* **10**, 18 (2010).
17. C. D. O'Donnell *et al.*, *Clin. Vaccine Immunol.* **21**, 737–746 (2014).
18. J. Wrammert *et al.*, *Nature* **453**, 667–671 (2008).
19. J. H. Kim, I. Skountzou, R. Compans, J. Jacob, *J. Immunol.* **183**, 3294–3301 (2009).
20. M. S. Miller *et al.*, *Sci. Transl. Med.* **5**, 198ra107 (2013).

21. D. J. Smith, S. Forrest, D. H. Ackley, A. S. Perelson, *Proc. Natl. Acad. Sci. U.S.A.* **96**, 14001–14006 (1999).
22. K. Pan, *PLOS ONE* **6**, e23910 (2011).
23. T. Francis Jr., J. E. Salk, J. J. Quilligan Jr., *Am. J. Public Health Nations Health* **37**, 1013–1016 (1947).
24. E. A. Belongia *et al.*, *J. Infect. Dis.* **199**, 159–167 (2009).
25. D. M. Skowronski *et al.*, *J. Infect. Dis.* **199**, 168–179 (2009).
26. C. B. Bridges *et al.*, *JAMA* **284**, 1655–1663 (2000).

ACKNOWLEDGMENTS

We thank R. Bodewes, J. Bryant, D. Burke, N. Lewis, E. Selkov, B. Mühlemann, G. de Mutsert, and F. Pistoor. We also thank the staff of the Ha Nam Provincial Preventive Medicine Centre, the Hamlet health workers, and the National Institute for Hygiene and Epidemiology, Vietnam, for their support in conducting the fieldwork. We are indebted to the cooperation of the Ha Nam cohort and vaccine study participants. J.M.F. is supported by a Medical Research Council Fellowship (MR/K021885/1) and a Junior Research Fellowship from Homerton College, L.C.K. by the Gates-Cambridge Scholarship and the NIH Oxford-Cambridge Scholars program, and C.A.R. by a Royal Society University Research Fellowship (RG55423). We acknowledge the National Institute of Allergy and Infectious Diseases–NIH Centers of Excellence for Influenza Research and Surveillance contracts HHSN266200700010C and HHSN272201400008C, Nederlandse Organisatie voor Wetenschappelijk Onderzoek VICI grant 91896613, the European Union FP7 programs EMPERIE (223498) and ANTIGONE (278976), Human Frontier Science Program grant P0050/2008, the Wellcome Trust (WT087982MA), and NIH Director's Pioneer Award DP1-OD000490-01. The Melbourne WHO Collaborating Centre for Reference and Research on Influenza is supported by the Australian government Department of Health. A.D.M.E.O. (as Chief Scientific Officer of Viroclinics Biosciences BV) has advisory affiliations with GlaxoSmithKline, Novartis, and Roche. Sequences of the influenza viruses used in this study are available in GenBank with accession numbers: KM821278 to KM821358. Erasmus Medical Center (Rotterdam, the Netherlands) requires a materials transfer agreement for sharing viruses and antisera.

SUPPLEMENTARY MATERIALS

www.sciencemag.org/content/346/6212/996/suppl/DC1
Materials and Methods
Supplementary Text
Figs. S1 to S49
Tables S1 to S14
References (*27*–*35*)

23 May 2014; accepted 3 October 2014
10.1126/science.1256427

INFLAMMATION

Nucleoside reverse transcriptase inhibitors possess intrinsic anti-inflammatory activity

Benjamin J. Fowler,[1,2] Bradley D. Gelfand,[1,3,4] Younghee Kim,[1] Nagaraj Kerur,[1] Valeria Tarallo,[1,5] Yoshio Hirano,[1] Shoba Amarnath,[6] Daniel H. Fowler,[6] Marta Radwan,[7] Mark T. Young,[7] Keir Pittman,[8] Paul Kubes,[8] Hitesh K. Agarwal,[9] Keykavous Parang,[9] David R. Hinton,[10] Ana Bastos-Carvalho,[1] Shengjian Li,[1] Tetsuhiro Yasuma,[1] Takeshi Mizutani,[1] Reo Yasuma,[1] Charles Wright,[1] Jayakrishna Ambati[1,2]*

Nucleoside reverse transcriptase inhibitors (NRTIs) are mainstay therapeutics for HIV that block retrovirus replication. *Alu* (an endogenous retroelement that also requires reverse transcriptase for its life cycle)–derived RNAs activate P2X7 and the NLRP3 inflammasome to cause cell death of the retinal pigment epithelium in geographic atrophy, a type of age-related macular degeneration. We found that NRTIs inhibit P2X7-mediated NLRP3 inflammasome activation independent of reverse transcriptase inhibition. Multiple approved and clinically relevant NRTIs prevented caspase-1 activation, the effector of the NLRP3 inflammasome, induced by *Alu* RNA. NRTIs were efficacious in mouse models of geographic atrophy, choroidal neovascularization, graft-versus-host disease, and sterile liver inflammation. Our findings suggest that NRTIs are ripe for drug repurposing in P2X7-driven diseases.

Nucleoside reverse transcriptase inhibitors (NRTIs) are widely used to treat HIV. Age-related macular degeneration (AMD) is a leading cause of blindness in the elderly population worldwide (*1*, *2*). In geographic atrophy, the late stage of the prevalent and untreatable dry form of AMD, overabundance of noncoding *Alu* RNAs is implicated in cell death of the retinal pigment epithelium (RPE) (*3*–*5*). Because *Alu* sequences are noncoding retrotransposons that, like HIV, rely on reverse transcriptase for their life cycle (*6*), we hypothesized that NRTIs could block *Alu* RNA–induced cytotoxicity. Multiple NRTIs are typically administered orally to HIV patients at a total NRTI dose of up to 15 mg kg^{-1} day^{-1} (*7*) [equivalent dose in mice: 185 mg kg^{-1} day^{-1} (*8*)]. A clinically relevant dose (single daily oral administration of 150 mg kg^{-1}) of the NRTI stavudine (d4T), which is U.S. Food and Drug Administration–approved for the treatment of HIV infection, prevented *Alu*-induced RPE degeneration (*4*, *5*) in wild-type mice (Fig. 1A). A lower dose of oral d4T (50 mg kg^{-1} day^{-1}) also prevented *Alu*-induced degeneration, as did twice daily intraperitoneal administration of 50 mg kg^{-1} of the NRTI zidovudine (AZT) (Fig. 1B and fig. S1).

Alu RNA induces RPE cell death via activation of caspase-1 by the innate immune complex known as the NLRP3 inflammasome (*5*, *9*). Western blotting of RPE lysates from d4T-treated mice confirmed that d4T blocked caspase-1 activation (fig. S2A). Caspase-1, in turn, cleaves pro-interleukin-18 (IL-18) into its mature form, which induces RPE degeneration via IRAK4 phosphorylation (*5*); d4T also blocked IL-18 maturation and IRAK4 phosphorylation in vivo (fig. S2A). Consistent with the notion that d4T prevents RPE degeneration upstream of IL-18 by blocking caspase-1 activation, the protective effect of d4T in *Alu*-treated mice was overridden by subretinal injection of recombinant mature mouse IL-18 (fig. S2B). d4T also prevented *Alu*-induced caspase-1 activation (*10*) and IRAK4 phosphorylation in primary human (Fig. 1C) and wild-type mouse RPE cells (fig. S2C) without reducing *Alu* RNA levels (fig. S2D). Other clinically relevant NRTIs, including lamivudine (3TC) and abacavir (ABC), similarly blocked caspase-1 cleavage induced by *Alu* RNA (Fig. 1D).

To determine whether reverse transcriptase inhibition was required for inflammasome blockade by d4T, we synthesized a 5′-*O*-methyl–modified version of d4T (me-d4T) (figs. S3 to S5). Only the triphosphate forms of nucleoside analogs inhibit reverse transcriptase; the methyl modification at the 5′ position prevents phosphorylation and thus formation of nucleoside triphosphate (*11*). As predicted, me-d4T, unlike d4T, did not inhibit lentiviral vector transduction of green fluorescent protein (GFP) (fig. S6, A and B). Moreover, the triphosphate metabolite of some dideoxy nucleoside analogs causes depletion of mitochondrial DNA (*12*); we found that d4T, but not me-d4T, reduced mtDNA levels in RPE cells (Fig. 2A). Notably, despite its inability to inhibit polymerases, me-d4T still blocked caspase-1 activation and IRAK4 phosphorylation by *Alu* RNA in RPE cells (Fig. 2B). We confirmed that me-d4T also prevented *Alu*-induced RPE degeneration in wild-type mice (Fig. 2C). These data suggest that d4T can block caspase-1 activation and RPE degeneration independent of reverse transcriptase inhibition.

We also tested whether NRTIs blocked NLRP3 inflammasome activation by lipopolysaccharide/adenosine 5′-triphosphate (LPS/ATP), which is not known to signal via reverse transcriptase (*13*). d4T inhibited LPS/ATP-induced caspase-1 maturation in primary mouse bone marrow–derived macrophages (BMDMs) (Fig. 3A). To demonstrate that

[1]Department of Ophthalmology and Visual Sciences, University of Kentucky, Lexington, KY 40536, USA. [2]Department of Physiology, University of Kentucky, Lexington, KY 40536, USA. [3]Department of Microbiology, Immunology, and Human Genetics, University of Kentucky, Lexington, KY 40536, USA. [4]Department of Biomedical Engineering, University of Kentucky, Lexington, KY 40536, USA. [5]Angiogenesis Lab, Institute of Genetics and Biophysics, CNR, Naples, Italy [6]Experimental Transplantation and Immunology Branch, National Cancer Institute, National Institutes of Health, Bethesda, MD, USA. [7]School of Biosciences, Cardiff University, Cardiff CF10 3AX, UK. [8]Immunology Research Group, University of Calgary, Calgary, Alberta T2N 4N1, Canada. [9]Chapman University School of Pharmacy, 9401 Jeronimo Road, Harry and Diane Rinker Health Science Campus, Irvine, CA 92618, USA. [10]Departments of Pathology and Ophthalmology, Keck School of Medicine of the University of Southern California, Los Angeles, CA 90033, USA.
***Corresponding author. E-mail: jamba2@email.uky.edu**

Science
AAAS

Antibody landscapes after influenza virus infection or vaccination

J. M. Fonville *et al.*

Science **346**, 996 (2014);
DOI: 10.1126/science.1256427

This copy is for your personal, non-commercial use only.

If you wish to distribute this article to others, you can order high-quality copies for your colleagues, clients, or customers by clicking here.

Permission to republish or repurpose articles or portions of articles can be obtained by following the guidelines here.

The following resources related to this article are available online at www.sciencemag.org (this information is current as of March 20, 2015):

Updated information and services, including high-resolution figures, can be found in the online version of this article at:
http://www.sciencemag.org/content/346/6212/996.full.html

Supporting Online Material can be found at:
http://www.sciencemag.org/content/suppl/2014/11/19/346.6212.996.DC1.html

A list of selected additional articles on the Science Web sites **related to this article** can be found at:
http://www.sciencemag.org/content/346/6212/996.full.html#related

This article **cites 34 articles**, 18 of which can be accessed free:
http://www.sciencemag.org/content/346/6212/996.full.html#ref-list-1

This article has been **cited by** 2 articles hosted by HighWire Press; see:
http://www.sciencemag.org/content/346/6212/996.full.html#related-urls

This article appears in the following **subject collections:**
Epidemiology
http://www.sciencemag.org/cgi/collection/epidemiology

Downloaded from www.sciencemag.org on March 20, 2015

Science (print ISSN 0036-8075; online ISSN 1095-9203) is published weekly, except the last week in December, by the American Association for the Advancement of Science, 1200 New York Avenue NW, Washington, DC 20005. Copyright 2014 by the American Association for the Advancement of Science; all rights reserved. The title *Science* is a registered trademark of AAAS.